crystals

MDPI

Article

Synthesis and Cap-Dependent Endonuclease Inhibition of Baloxavir Derivatives

Yiyun Wang [1,2], Jiaru Wang [1,†], Hui Wu [2], Longyao Cui [2], Zihui Meng [1], Zhibin Xu [1,*], Zhonghui Zheng [2,*] and Jiarong Li [1]

[1] School of Chemistry and Chemical Engineering, Beijing Institute of Technology, Beijing 100081, China; wyy4184@126.com (Y.W.); 3120201380@bit.edu.cn (J.W.); mengzh@bit.edu.cn (Z.M.); jrli@bit.edu.cn (J.L.)
[2] Shandong Xinhua Pharmaceutical Co., Ltd., No. 1 Lutai Avenue, Zibo 255086, China; wuhuichem@126.com (H.W.); 18766422180@163.com (L.C.)
* Correspondence: zbxu@bit.edu.cn (Z.X.); zhengzhonghui@sina.com (Z.Z.)
† Jiaru Wang is contributed equally to this work.

Abstract: Baloxavir marboxil is a creative antiviral drug for influenza A and B viruses with a novel mechanism of action. In this study, three series comprising a total of 21 previously unreported target compounds were designed and synthesized. The drug-likeness of these compounds was evaluated by molecular docking, PAINS-Remover and SwissADME. The inhibitory effect and affinity of the compounds on the cap-dependent endonuclease activity of the influenza virus were evaluated. Compounds **I-4, II-1~II-9** and compound **III-8** showed similar inhibitory activity to baloxavir (7.45 μM) on the cap-dependent endonuclease. In particular, compounds **I-4** (3.29 μM) and **II-2** (1.46 μM) showed strong cap-dependent endonuclease inhibitory activity. The structure–activity relationship studies showed that the inhibitive effect of the compounds on endonuclease was enhanced when the dibenzothiepin rings were substituted by diphenylmethyl containing chiral-center electron-withdrawing groups, dibenzocycloheptane, dihydrodibenzo[b,e]oxepin, and five-member heterocycles containing aryl substitution.

Keywords: baloxavir; derivatives; synthesis; inhibition

check for updates

Citation: Wang, Y.; Wang, J.; Wu, H.; Cui, L.; Meng, Z.; Xu, Z.; Zheng, Z.; Li, J. Synthesis and Cap-Dependent Endonuclease Inhibition of Baloxavir Derivatives. *Crystals* **2023**, *13*, 988. https://doi.org/10.3390/cryst13070988

Academic Editors: Matthew Groves and Abel Moreno

Received: 7 April 2023
Revised: 19 June 2023
Accepted: 19 June 2023
Published: 21 June 2023

Copyright: © 2023 by the authors. Licensee MDPI, Basel, Switzerland. This article is an open access article distributed under the terms and conditions of the Creative Commons Attribution (CC BY) license (https://creativecommons.org/licenses/by/4.0/).

1. Introduction

Influenza is one of the greatest challenges facing humanity [1,2]. For illnesses caused by the influenza virus, vaccines and drugs are still the main treatment. Influenza vaccines exert protective effects only against the antigens of the influenza virus strains of the current epidemic because of the frequent variation in influenza viruses. When a new strain of influenza virus with a large variation appears, the body does not produce the corresponding antibodies. Because there is no corresponding vaccine or drugs, the new flu will sweep the world, bringing death and huge economic losses. According to historical statistics, pandemic influenza outbreaks occur once about 25 years [3].

Currently, the main anti-influenza drugs on the market include neuraminidase inhibitors, ion channel blockers and so on [4–8]. However, with the widespread use of these drugs, influenza viruses have developed drug resistance [9], especially highly therapeutic and resistant influenza strains such as H1N1 [10], H5N1 [11], and H7N9 [12], which have caused severe infections worldwide [13]. Because of the continuous variation and recombination of influenza viruses, medical chemists have explored anti-influenza drugs for new targets or mechanisms of action [14–17].

In March 2018 and October 2018, baloxavir marboxil (trade name: Xofluza) was launched in Japan and the United States, respectively. Unlike neuraminidase inhibitors, which prevent the release of progeny virions from infected host cells, baloxavir marboxil is a novel cap-dependent endonuclease (CEN) protein inhibitor within the polymerase acidic protein (PA) subunit of influenza A and B viruses that blocks influenza virus proliferation

by inhibiting the initiation of mRNA synthesis [18–21]. In non-clinical studies, baloxavir has shown good antiviral effects against most influenza viruses, including oseltamivir-resistant strains. Baloxavir is also one of the few new drugs in the world that can inhibit the proliferation of influenza viruses [22]. Moreover, compared with oseltamivir that needs to be taken for five days, only a single oral dose of baloxavir marboxil could alleviate the symptoms of influenza [23].

As a novel antiviral drug with a new mechanism of action against influenza A and B viruses, baloxavir marboxil has a broad market prospect [24,25]. Some medical chemists have begun to study the derivatives and the structure–activity relationship of baloxavir.

Tang Changhua [26] designed a series of derivatives by optimizing the dibenzothiepin structure, and the synthetic and biological activity of the compounds were tested. These compounds include dibenzocycloheptene pentacyclic heterocyclic structures, dibenzothiepin structures containing benzene ring substitution, and benzonaphthothiophene structures. The antiviral activity and cytotoxicity tests of these 38 compounds showed that these compounds have excellent antiviral activity, with an EC50 of less than 0.1 μM against the influenza virus (HIN1). Tang Lin [27] designed and synthesized a series of novel substituted polycyclic pyridinone derivatives, and tested their anti-influenza virus activity. Cytopathic effects and cytotoxicity tests demonstrated that all the compounds showed strong anti-influenza virus activity and low cytotoxicity. Some of these compounds effectively inhibited influenza A virus replication at picomolar concentrations. No groups were introduced to the dibenzocycloheptene ring, and the antiviral activity was the most effective. Miyagawa [28] discovered a series of endonuclease inhibitors (such as AV5116) with good biological activity by modifying different substituents on the nitrogen atom of the triazine ring during the process of optimizing the structure of baloxavir. Its IC50 value for inhibiting endonuclease was able to reach 0.286 μM.

In order to find more effective CEN inhibitor compounds and determine the structure–activity relationship of baloxavir, three series of new baloxavir derivatives were designed and synthesized, and their biological activities are studied in this paper.

2. Materials and Methods

2.1. Instruments and Reagents

Chemicals and reagents were purchased from Sinopharm Group Chemical Reagent Co., Ltd. (Shanghai, China), Le Yan Chemical Reagent Co., Ltd. (Shanghai, China), and Macklin (Shanghai, China), analytically pure. The remaining materials were provided by Shandong Xinhua Pharmaceutical Co., Ltd. (Zibo, China). A circulating water vacuum pump (SHB-III, Zhengzhou Great Wall Science, Industry and Trade Co., Ltd., Zhengzhou, China), an electric blast drying oven (GZX-9240MBE, Shanghai Boxun Industrial Co., Ltd., Shanghai, China), an electronic balance (PB3002-S, METTLER TOLEDO, Switzerland), a constant temperature magnetic stirrer (DF-101S, Zhengzhou Great Wall Industry and Trade Co., Ltd., Zhengzhou, China), a three-purpose UV instrument (ZF-2, Shanghai Anting Electronic Instrument Factory, Shanghai, China), a high-performance liquid chromatography (Agilent-1200, Agilent Technologies 23 Mill Street, Arcade, CA, USA), a Bruker nuclear magnetic resonance instrument (400, 600, 100, and 150 MHz), and a Bruker mass spectrometer (Germany).

2.2. General Synthetic Method for the Compounds

2.2.1. Synthetic Method for the Compounds **I**

7-(benzyloxy)-3,4,12,12a-tetrahydro-1H-[1,4]oxazino[3,4-c]pyrido[2,1-f][1,2,4]triazine-6,8-dione (Compound **a**) and diphenylcarbinol were introduced into a thick-walled pressure bottle, and then T_3P ethyl acetate solution and HND-580 were added. The reaction was carried out at 100 °C for 12 h. After the reaction was completed, the intermediate was obtained through extraction, washing, drying and evaporation under reduced pressure. The obtained intermediate was transferred to the reaction flask, then DMAc and lithium chloride were added into the reaction mixture. The reaction was stirred at 70 °C for 8 h

and the target product (**I-1~I-4**) was obtained through extraction, washing, drying and evaporation, and purified by column chromatography (Figure 1).

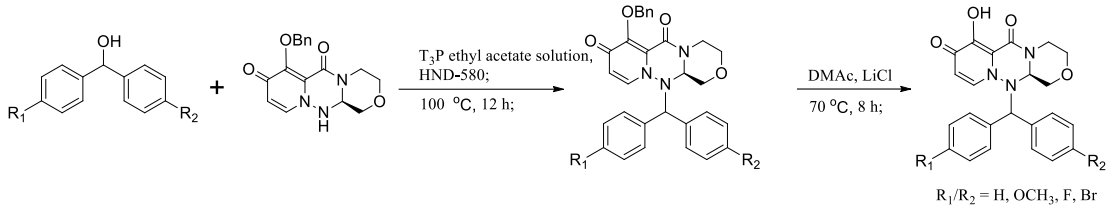


Figure 1. Synthesis route of series **I** target compounds.

2.2.2. Synthetic Method for the Compounds **II**

Compound **a** and the corresponding 7-membered heterocyclic compound were added to the thick-walled pressure bottle, and then T_3P ethyl acetate solution and HND-580 were added. The reaction was at 100 °C for 12 h. After the reaction was completed, the intermediate was obtained through extraction, washing, drying and evaporation. The obtained intermediate was transferred to the reaction flask, then DMAc and lithium chloride were added to the reaction mixture. The temperature was raised to 70 °C and maintained for 8 h. After the reaction was completed, the target product (**II-1~II-9**) was obtained through extraction, washing, drying, evaporation and column chromatography (Figure 2).

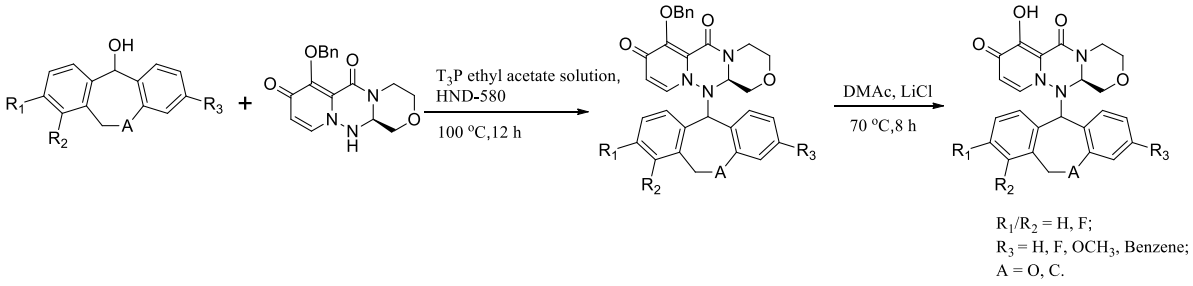


Figure 2. Synthesis route of series **II** target compounds.

2.2.3. Synthetic Method for the Compounds **III**

Compound **a** and the corresponding chloromethyl pentane heterocyclic compound were added to the flask, and then DMF and potassium carbonate were added. The temperature was raised to 45 °C for a stirring reaction. The reaction was detected by TLC. After the reaction was completed, the intermediate was obtained by extraction, washing, drying, and evaporation. The obtained intermediate was added to the reaction flask, then DMAc and lithium chloride were added into the reaction mixture. The temperature was raised to 70 °C for a closed stirring reaction. The reaction was detected by TLC. After the reaction was completed, the target product (**III-1~III-8**) was obtained by extraction, washing, drying and evaporation (Figure 3).

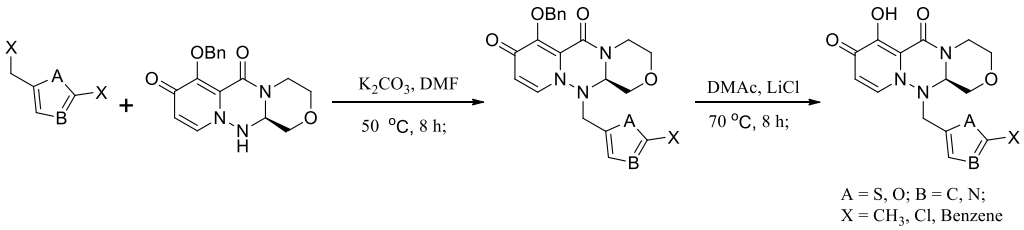


Figure 3. Synthesis route of series **III** target compounds.

2.3. Drug Likeness

In order to determine whether the target compounds designed in this paper contain false positive compounds, a PAINS-remover was used to perform virtual screening on all

the target compounds in this paper. In order to predict the rationality of the target compounds, Lipinski rule analysis was used. Concurrently, SwissADME was used to analyze the druggability, pharmacokinetics, drug similarity, and pharmacochemical friendliness of the compounds. The chemical composition was screened through the Swiss ADME online platform (http://swissadme.ch/, 25 September 2022), and conditions were set: GI absorption was "High", 2 and more than 2 of the 5 drug types (Lipinski, Ghose, Veber, Egan, Muegge) were "Yes", and oral bioavailability, (OB) $\geq$ 30% and druglikeness (DL) $\geq$ 0.18.

2.4. Biological Activity of the Synthesized Baloxavir Derivatives

2.4.1. Establishment of a Test Method for Endonuclease Inhibitory Activity

The recombinant protein (100 μg CSB-YP395880ILR1) was purchased from Wuhan Huamei Bioengineering Co., Ltd. (Wuhan, China). It was used directly without purification.

Details are as follows:

Species: Influenza A virus (strain A/USA: Huston/AA/1945 H1N1)

Expression area: 1–209aa

Protein label: N-terminal 6×His-tagged

Expression host: yeast

Molecular weight: 26.6 kDa

Amino acid sequence:

MEDFVRQCFNPMIVELAEKAMKEYGEDLKVETNKFAAICTHLEVCFMYSDFHFI-NEQGESIIVELGDPNALLKHRFEIIEGRDRTMAWTIVNSICNTTGAEKPKFLPDLYDYK-ENRFIEIGVTRREVHIYYLEKANKIKSEKTHIHIFSFTGEEMATKADYTLDEESRARIKTR-LFTIRQEMASRGLWDSFRQSERGEETIEERFEITG

Fluorescent probe

Sequence and marker: 5′-6FAM-TGGCAATATCAGCTCCACA-MGBNFQ-3′

5′-Fluorescent label: Fluorophore 6-carboxyfluorescein (6-FAM) (492 nm/518 nm)

3′-Fluorescent label: Minor groove binder non-fluorescent quencher

Determine the enzymatic reaction time (pre experiment):

The experiment was divided into two groups: the reaction group and the control group. The reaction group used PA protein as a catalytic enzyme, while the control group used bovine serum albumin (BSA) as a catalytic enzyme. The reaction system was established according to Table S1 (see Supplementary Materials), and fluorescence signals were collected every 1 min from 0 min to 180 min. The fluorescence signal value was fitted to a logarithmic growth curve. The time at which the fluorescence amount was first higher than or equal to the cut-off threshold (maximum) was determined as the starting point of the reaction platform period. Each group contained three repeated tests.

The optimal enzymatic reaction time was set as the reaction time, and the concentration gradient was set for enzyme activity comparison. The experimental group included a compound group (a total of 8 groups were established with a compound concentration gradient, and the final concentration was 1 μM, 5 μM, 25 μM, 50 μM, 100 μM, 200 μM), a positive control and a negative control. The reaction system method was established according to the components in Table S2.

During the construction of the system, components other than the probe were added first, and then the probe was added after incubation at 37 °C for 30 min. Subsequently, timing monitoring of fluorescence changes was started. The signal collection time was the optimal reaction time described in the previous step, and each group contained three repeated tests. The tests were conducted in a dark water bath at 37 °C. Ensight was used to measure and collect recorded data. A 488 nm wavelength laser was used as the excitation light during fluorescence-signal measurement, and fluorescence-intensity readings at the 518 nm wavelength were collected.

2.4.2. Affinity Test of Compounds to Endonucleases

To optimize the conditions to couple the endonuclease onto the chip, 100 μg PA protein was dissolved in 1 mL of deionized water to obtain 100 μg/mL PA protein solution. The

100 μg/mL PA protein solution was diluted with a 10 mM sodium acetate coupling buffer (pH 4.5) to 40 μg/mL, and the contact time was 600 s. The endonuclease was coupled to the CM5 chip using an SPR molecular interaction instrument (Biocore T200, MA, USA). Because these compounds were insoluble in water, calibration of the DMSO solvent data was required. The response values of the compounds at different concentrations were measured using an SPR molecular interaction instrument (Biocore T200). The values of ka and kd (ka is the affinity constant, kd is the dissociation constant) of the compound to the endonuclease were measured using an SPR molecular interaction instrument, and then the affinity KD was calculated. KD = kd/ka, the unit of KD is M (mol/L).

2.5. Molecular Docking Study

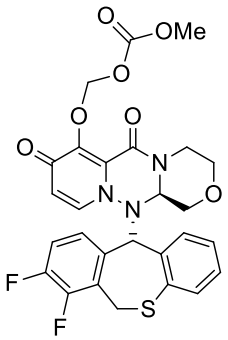
The target compounds with good inhibition were selected for a molecular docking study to explore and simulate the binding relationship between these synthesized compounds and the receptor (protein). Pymol software was used for mapping and interaction force analysis. The crystal complex structure with ligand BXA (PDB ID: 6FS6) was downloaded from the PDB database and imported into chimera to delete the molecules unrelated to binding (such as residues, OH, coenzymes and surfactants, etc.), and the protein structure file for molecular docking was obtained through hydrogenation and charge processing. MarvinSketch(Shanghai Budou Information Technology Co., Ltd., Shanghai, China) was used to build the structure of small molecules and perform pre-docking processing. Finally, Ledock software(Lephar, Shanghai, China) was used for molecular docking.

3. Results and Discussion

3.1. Design and Synthesis

Diaryl methanol compounds, five-membered heterocyclic and seven-membered heterocyclic compounds containing heteroatoms such as nitrogen, oxygen and sulfur were the sources of many active small-molecular compounds. Drugs containing these structural fragments have also been continuously developed, such as new anti-HIV drugs, anti-hepatitis drugs and anti-bacterial drugs. They play a key role in the pharmacological activity of drugs for the prevention or treatment of diseases, and have also received extensive attention in pharmaceutical chemistry and molecular design.

Baloxavir marboxil (Figure 4) is a prodrug, and its active substance is baloxavir. Baloxavir marboxil can only exert its anti-influenza effect after being hydrolyzed into baloxavir in the body. The pharmacophore of baloxavir is 7-(benzyloxy)-3,4,12,12a-tetrahydro-1H-[1,4]oxazole[3,4-c]pyrido[2,1-f][1,2,4]triazine-6,8-dione (Compound **a**), which is a structural fragment that exhibits physical and chemical characteristics necessary for specific biological activity. The polycyclic pyridone scaffold of baloxavir associated with antiviral activity cannot be modified randomly. The dibenzothiepin ring, the rigidity of which seems to be related to the antiviral activity, can be modified to increase its rigidity, such as by dibenzothiepin derivatives, polycyclic pyridinone derivatives and AV5116 (Figure 5).



Baloxavir marboxil

Figure 4. Baloxavir marboxil.

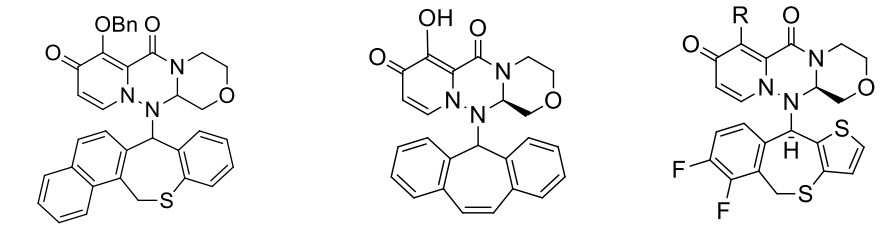


Figure 5. Endonuclease inhibitors with good biological activity.

In this paper, the combination principle, bioisostere and skeleton transition strategy were used to optimize the structure of dibenzothiepin by taking baloxavir as the lead compound. The dibenzothiepin was replaced by diaryl carbinol compounds, 5-membered heterocyclic compounds containing nitrogen, oxygen and sulfur, and 7-membered heterocyclic compounds, respectively. A total of 3 series of 21 target compounds were designed, including dibenzyl carbinol compounds, dibenzoyl 7-membered heterocyclic compounds and 5-membered heterocyclic compounds (Figure 6).

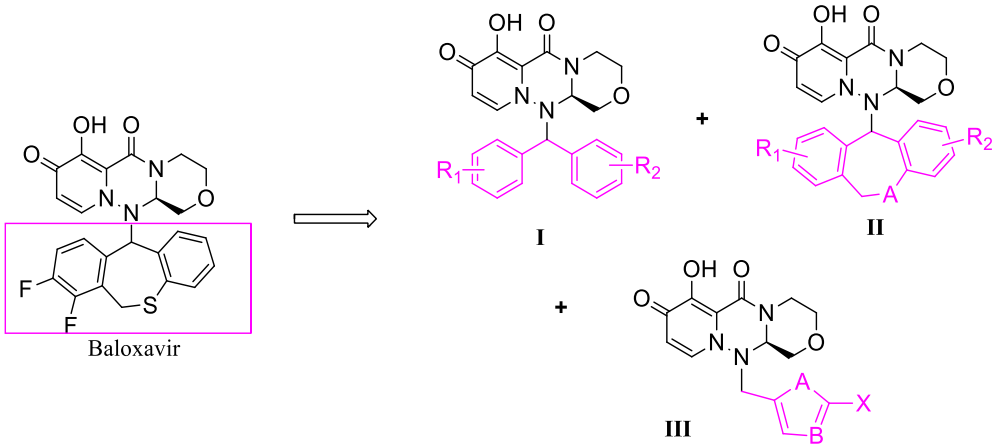
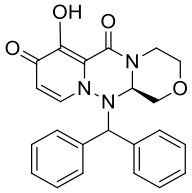
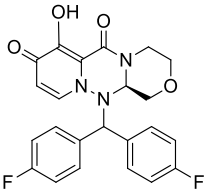
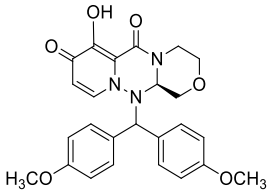
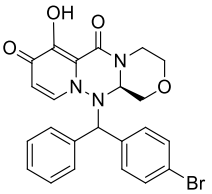


Figure 6. Structural Design of Baloxavir Derivatives. Note: The dibenzothiepin was replaced by diaryl carbinol compounds, 5-membered heterocyclic compounds and 7-membered heterocyclic compounds, respectively. In series **I**, R_1/R_2 = H, OCH_3, F, Br. In series **II**, R_1/R_2 = H, F; R_3 = H, F, OCH_3, Benzene; A = O, C. In series **III**, A = S, O; B = C, N; X = CH_3, Cl, Benzene.

In this study, the series **I** target compounds were designed by replacing the dibenzothiepin structure of baloxavir with a diphenylcarbinol compound. Diphenylcarbinol compounds selected from series **I** target compounds are common structures in pharmaceutical chemistry, including diphenylcarbinol, 4,4′-dimethoxy-diphenylcarbinol, 4,4′-difluorodiphenylcarbinol, 4-bromodiphenylcarbinol and so on. This paper primarily investigates the effects of diphenylcarbinol compounds R1 and R2 as electron donor and electron attractor groups in pharmacological activities. Additionally, the impact of the chiral center on activity was examined. The R1 and R2 substituents were selected from hydrogen, methoxy, fluorine, bromine, etc. Four diphenylcarbinol compounds (**I-1~I-4**) with different R1 and R2 substituents were designed, all of them new compounds that have not been reported previously (Table 1). All the compounds were successfully synthesized and characterized with different spectroscopic techniques.

Table 1. Structures of the synthesized compounds **I**.

Number	Structure	Number	Structure
I-1		**I-3**	
	$C_{23}H_{21}N_3O_4$; Mw: 403.43		$C_{23}H_{19}F_2N_3O_4$; Mw: 439.41
I-2		**I-4**	
	$C_{25}H_{25}N_3O_6$; Mw: 463.48		$C_{23}H_{20}BrN_3O_4$; Mw: 482.32

Sulfur in dibenzothiepin is a divalent electron, and the O, S, NH, CH and other divalent atoms or groups can be exchanged. Therefore, the A of series **II** target compounds could be O and C. The selected seven-membered heterocyclic rings are common structures in pharmaceutical chemistry, including dibenzo-cycloheptene, dibenzocycloheptane and dihydrodibenzo[b,e]oxepin. The primary aim in selecting heptadibenzo heterocyclic substituents was to explore the effect of these compounds on pharmacological activity when R1, R2, and R3 are hydrogen, electron-donating, and electron-withdrawing groups. The effect of R3 on pharmacological activity in different locations was also explored. The substituents R1 and R2 were selected from hydrogen, fluorine, and so on. Fluorine and hydrogen atoms are one valence electrons, which can be replaced with each other. Fluorine and hydrogen atoms are very similar in size and radius to van der Waals forces. Secondly, fluorine is the most electronegative atom of the halogens and forms a very stable bond with carbon, so fluorine derivatives are more stable for metabolic degradation. In addition, since fluorine has no vacant d orbital, it cannot form a resonance with the electron donor. Because of the above particularity of the fluorine atom, F is often used to replace H in drug design to improve its metabolic stability. R3 substituents were selected from hydrogen, fluorine, methoxy, benzene ring, etc. Methoxy was for electron donor groups, F was for the electron-absorbing group, the benzene ring was the large π bond, with six centers and six electrons, that can be regarded as a buffer system, that is, it could suck electrons in and could also give electrons. R3 could be anywhere on the benzene ring. Nine different dibenzo seven-membered heterocyclic compounds (**II-1~II-9**) were designed, all of which were new compounds that had not been reported before (Table 2). All the compounds were successfully synthesized and characterized with different spectroscopic techniques.

Table 2. Structures of the synthesized compounds **II**.

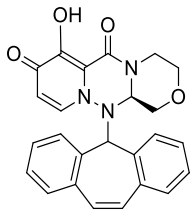
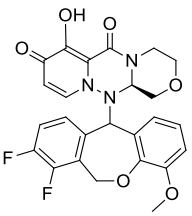
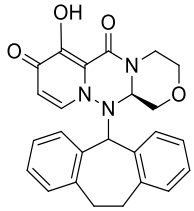
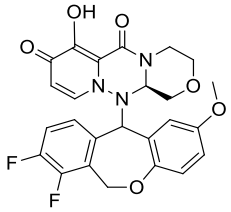
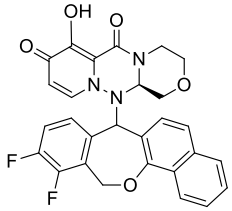
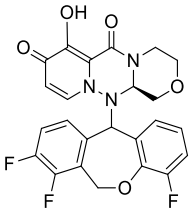
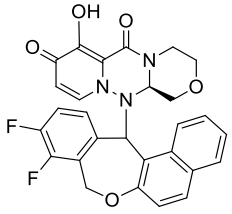
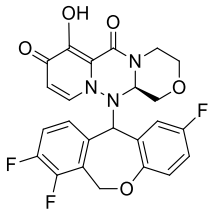
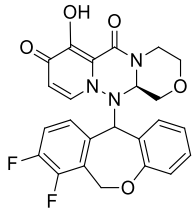
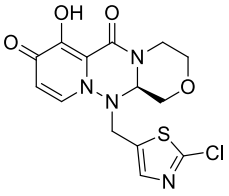
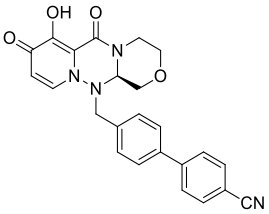
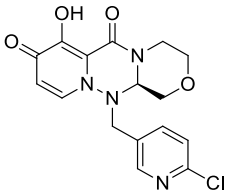
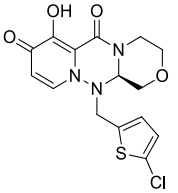
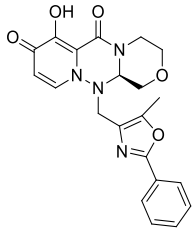
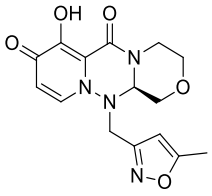
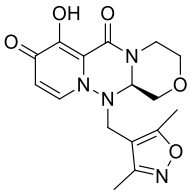
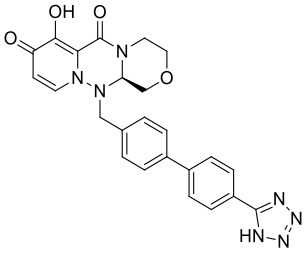
Number	Structure	Number	Structure
II-1		**II-6**	
	$C_{25}H_{21}N_3O_4$; Mw: 427.45		$C_{25}H_{21}F_2N_3O_6$; Mw: 497.44

Table 2. *Cont.*

Number	Structure	Number	Structure
II-2	 $C_{25}H_{23}N_3O_4$; Mw: 429.46	**II-7**	 $C_{25}H_{21}F_2N_3O_6$; Mw: 497.44
II-3	 $C_{28}H_{21}F_2N_3O_5$; Mw: 517.48	**II-8**	 $C_{24}H_{18}F_3N_3O_5$; Mw: 485.41
II-4	 $C_{28}H_{21}F_2N_3O_5$; Mw: 517.48	**II-9**	 $C_{24}H_{18}F_3N_3O_5$; Mw: 485.41
II-5	 $C_{24}H_{19}F_2N_3O_5$; Mw: 467.42		

Based on the skeleton transition strategy, the dibenzothiepin structure was simplified while the pharmacophore compound **a** of baloxavir remained unchanged. The dibenzothiepin structure was replaced by heterocyclic structures such as a thiazole ring or benzothiazole. The series **III** target compounds were designed to obtain novel compounds with more prominent activity. The heterocyclic compounds selected in series **III** are common structures in pharmaceutical chemistry, including thiazole, oxazole, imidazole, thiophene, pyridine, etc., mainly to explore the effects of five-member heterocyclic compounds on pharmacological activity when A and B were oxygen, sulfur and carbon and X was methyl, halogen and the benzene ring. Among other options, the A of series **III** target compounds could be S and O, B could be C and N, and X was selected from methyl, chlorine and the benzene ring, etc. Eight different five-membered heterocyclic compounds (**III-1~III-8**) were designed, all of them new compounds that had not been reported before (Table 3). All the compounds were successfully synthesized and characterized with different spectroscopic techniques.

Table 3. Structures of the synthesized compounds **III**.

Number	Structure	Number	Structure
III-1	 $C_{14}H_{13}ClN_4O_4S$; Mw: 368.79	**III-5**	 $C_{24}H_{20}N_4O_4$; Mw: 428.44
III-2	 $C_{16}H_{15}ClN_4O_4$; Mw: 362.76	**III-6**	 $C_{15}H_{14}ClN_3O_4S$; Mw: 367.80
III-3	 $C_{21}H_{20}N_4O_5$; Mw: 408.40	**III-7**	 $C_{15}H_{16}N_4O_5$; Mw: 332.31
III-4	 $C_{16}H_{18}N_4O_5$; Mw: 346.33	**III-8**	 $C_{24}H_{21}N_7O_4$; Mw: 471.47

3.2. Drug Likeness

PAINS-remover was used to carry out a virtual screening of all the target compounds in this study, and the retrieval results showed that none of the 21 target compounds was false positive.

In this paper, a total of 21 target compounds were analyzed by Lipinski's rule. Through the analysis of molecular weight, Clog P, the hydrogen bond receptor, the hydrogen bond donor and the number of rotatable bonds, the molecular weight of all compounds was between 300 and 500 (because naphthalene rings, molecular weight of **II-3** and **II-4** were 517.48, slightly larger than 500), the number of rotatable bonds ≤ 3, the number of hydrogen bond donors < 3, the number of hydrogen bond receptors < 10, Clog P < 5. The designed target compounds comply with Lipinski's rule basically, indicating that all target compounds designs may be reasonable).

The SwissADME program was used to analyze water solubility, pharmacokinetics, bioavailability and synthetic feasibility. All the 21 target compounds showed good drug-like properties. According to the retrieval results, all the target compounds were well absorbed in the gastrointestinal tract. Bioavailability was consistent with that of Baloxavir. The synthetic feasibility was comparable to that of baloxavir, which is of medium difficulty.

3.3. Biological Activity of the Synthesized Baloxavir Derivatives

3.3.1. The Affinity of the Target Compound to Endonuclease

The dissociation constant (kd) reflects the affinity of the compound to the target, and the smaller the value, the stronger the affinity. Conversely, the affinity constant (ka) exhibits an opposite relationship, higher values signify stronger affinity. The reaction affinity (KD = kd/ka) denotes that the larger the value, the more the drug concentration required to cause the maximum effect, and the smaller the affinity. So high affinity is a high binding constant and low dissociation constant.

As can be seen from Table 4, the ka and kd values of series **I** compounds were on the same order of magnitude as baloxavir, and KD values of series **I** compounds were also comparable to baloxavir, indicating that the affinity of series **I** compounds with endonuclease was similar to baloxavir. The affinity between the compound and the enzyme was related to bonding, three-dimensional conformation and spatial distance. The diphenyl methyl structure of compounds **I-1~I-3** was symmetrical, with low steric hindrance, and could be combined well with the enzyme. However, compound **I-4** has stereoisomerism, resulting in slightly reduced affinity for the enzyme compared to the other three compounds.

Table 4. Compound affinity to endonuclease.

Compound	ka (1/Ms)	kd (1/s)	KD (M)	Rmax (RU)
Baloxavir	689.0	0.04627	6.72×10^{-5}	156.6
I-1	338.0	0.0273	8.08×10^{-5}	233.4
I-2	248.7	0.008723	3.51×10^{-5}	3.93×10^{2}
I-3	138.7	0.03813	2.75×10^{-4}	2.38×10^{2}
I-4	194.8	0.05099	2.62×10^{-4}	3.97×10^{2}
II-1	332.3	0.008742	2.63×10^{-5}	491.2
II-2	275.5	0.01892	6.87×10^{-5}	273.2
II-3	596.3	0.07436	1.25×10^{-4}	690.2
II-4	2.587	7.15×10^{-6}	2.76×10^{-6}	2.18×10^{4}
II-5	999.7	0.1065	1.07×10^{-4}	144.4
II-6	88.50	0.02391	2.70×10^{-4}	374.5
II-7	651.0	0.04824	7.41×10^{-5}	127.6
II-8	2.152	7.29×10^{-2}	3.39×10^{-2}	1573
II-9	272.1	0.04264	1.57×10^{-4}	3.23×10^{2}
III-1	334.6	0.07437	2.22×10^{-4}	3.77×10^{2}
III-2	6.248×10^{4}	0.01521	2.43×10^{-7}	5.19×10^{-2}
III-3	3103	0.08764	2.83×10^{-5}	38.71
III-4	4.936×10^{5}	0.08729	1.77×10^{-7}	3.689
III-5	848.4	0.03766	4.44×10^{-5}	217.9
III-6	843.4	0.07487	8.88×10^{-5}	53.76
III-7	6.220×10^{4}	0.001021	1.64×10^{-8}	0.08219
III-8	6568	0.0698	1.06×10^{-5}	155.2

Series **II** target compounds demonstrated good endonuclease affinity. The KD values of **II-1**, **II-2**, **II-4** and **II-7** were comparable to or better than that of baloxavir, indicating that these compounds shared similar endonuclease affinity with barloxavir. Because the dibenzo seven-membered rings do not contain substituent groups and heteroatoms, compounds **II-1** and **II-2** have symmetrical structures and minor steric hindrance, allowing effective enzyme binding. However, due to their spatial conformation, **II-4** and **II-7** can combine well with enzymes. Other compounds exhibited slightly less affinity than baloxavir due to their three-dimensional conformation and steric hindrance.

For series **III** compounds, the five-membered heterocyclic compounds exhibited small structures, planar spatial conformations, and almost no steric hindrance, enabling effective enzyme binding. As shown in Table 4, compound **III-1** had a slightly lower ka value than baloxavir, whereas compound **III-2~III-8** demonstrated a larger ka value than baloxavir,

indicating stronger enzyme binding. Simultaneously, the kd values of **III-2~III-8** were comparable to that of baloxavir, signifying similar dissociation capabilities. The KD values of compounds **III-2~III-8** were all smaller than that of baloxavir, suggesting that their endonuclease affinity was superior to that of baloxavir.

Among the three series of compounds, the series **III** compounds exhibited virtually no steric hindrance due to their planar structure and could combine well with enzymes. The series **I** compounds had a symmetrical structure, minor steric hindrance, and could combine well with enzymes. However, the affinity of series **II** compounds was slightly lower than that of baloxavir due to the effect of the three-dimensional conformation and steric hindrance.

3.3.2. Inhibition of Target Compounds on Endonuclease

According to the reaction system, the optimal reaction time test sample was constructed. In the reaction process, the fluorescence signal in the reaction group was gradually enhanced with the passage of time. According to the fitting curve, 60 min was selected as the most appropriate time for the reaction, and the fluorescence signal curve is shown in Figure 7.

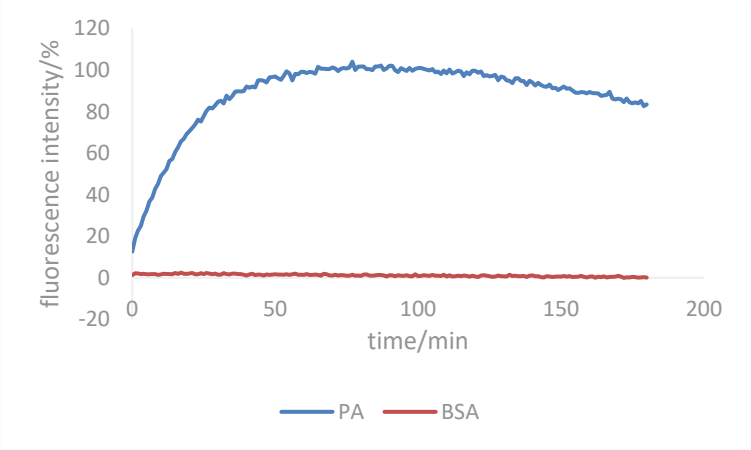


Figure 7. Enzymatic reaction time.

The test results for cap-dependent endonuclease activity inhibition by the target compounds are shown in Table 5. The IC50 value reflected the concentration of the drug that is required for 50% inhibition of cap-dependent endonuclease, with lower values representing better inhibition. As seen in Table 5, the IC50 value of baloxavir for endonuclease was 7.45 μM. The IC50 values for compounds **I-1** (18.74 μM), **I-2** (26.78 μM), and **I-3** (30.45 μM) were slightly larger than that of barloxavir, but within the same order of magnitude. The IC50 value of compound **I-4** (3.29 μM) on endonuclease was lower than that of baloxavir, indicating that compound **I-4** contained electron-absorbing groups and had chiral centers, which increased the interaction with the endonuclease, and the inhibition of cap-dependent endonuclease activity was better than that of baloxavir. The IC50 values of series **II** compounds on endonuclease were similar to that of barloxavir, within the same order of magnitude. The inhibitory activities of **II-3** and **II-4**, **II-6** and **II-7**, and **II-8** and **II-9** were nearly identical, indicating that the different positions of substituents had little effect on activity. Compound **II-2** (1.46 μM), with a dibenzocycloheptane structure and no substituents, exhibited increased endonuclease binding and enhanced inhibition compared to barloxavir (7.45 μM). **III-1**, **III-2**, **III-4** and **III-7** of series **III** compounds had no inhibitory effect on cap-dependent endonuclease activity. The IC50 values of **III-3**, **III-5**, **III-6**, and **III-8** were similar to that of barloxavir, within the same order of magnitude. The IC50 value of compound **III-8** (6.86 μM) was similar to that of baloxavir, and the structure of tetrazolium enhanced the binding to the endonuclease and the inhibition of the endonuclease.

Table 5. Inhibitory effect of target compounds on endonucleases.

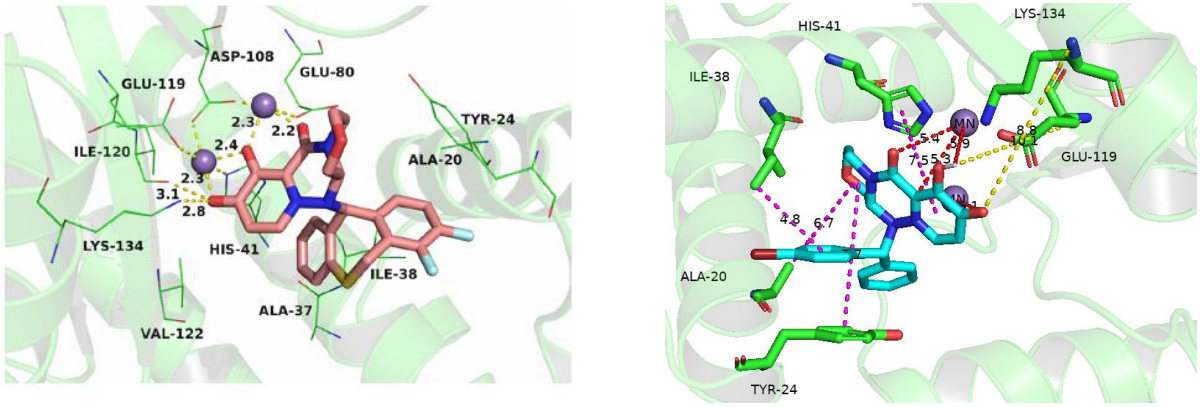
Compound	IC50 (μM)	Compound	IC50 (μM)
Baloxavir	7.45	**II-7**	5.46
I-1	18.74	**II-8**	6.83
I-2	26.78	**II-9**	8.54
I-3	30.45	**III-1**	0
I-4	3.29	**III-2**	0
II-1	8.07	**III-3**	13.7
II-2	1.46	**III-4**	0
II-3	5.46	**III-5**	7.37
II-4	8.46	**III-6**	50.55
II-5	6.62	**III-7**	0
II-6	5.23	**III-8**	6.86

Compared with the three series of compounds, the inhibition of cap-dependent endonuclease activity of series **II** compounds was much better than that of the other two series, which was closely related to the structure of the compounds. The structure of series **II** compounds was similar to that of baloxavir, which can interact well with the endonuclease and thus produce an inhibitory effect. Because of the chiral center and the optimal spatial conformation, **I-4** of the series **I** compound could also inhibit the endonuclease well. **III-1**, **III-2**, **III-4**, and **III-7** of series **III** compounds could not effectively interact with the endonuclease because they were on the same plane and could not inhibit cap-dependent endonuclease activity. Compounds **III-3**, **III-5** and **III-8** connected to the benzene ring and possessing specific conformations, could generate some interaction with the endonuclease, among which compounds **III-5** and **III-8** exhibited an inhibitory effect on the endonuclease similar to that of baloxavir.

3.4. Molecular Docking

Target compounds with good inhibition were selected for molecular docking studies based on the test results of cap-dependent endonuclease activity inhibition. Pymol was used for mapping and interaction force analysis.

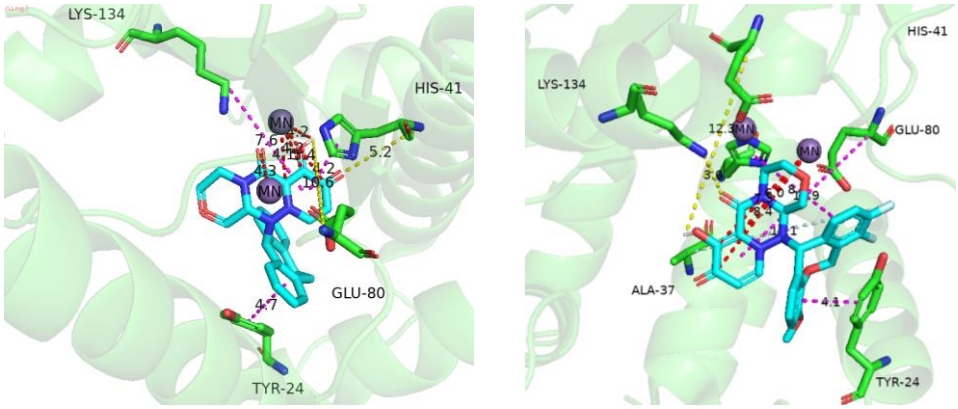
The optimal conformation of compound **I-4** and its binding force of the receptor protein were analyzed and compared with the molecular docking results of baloxavir, as shown in Figure 8. The binding energy of baloxavir to the enzyme was −7.44 kcal/mol, while the binding energy of compound **I-4** to the enzyme was −7.75 kcal/mol. The interaction between baloxavir and the endonuclease was nearly the same as **I-4**. In the molecular docking of compound **I-4**, the combination of OH in the pharmacophore with the NH_2 group on Glu119 to form a hydrogen bond, the carbonyl group also combined with the NH_2 group on Lys134 to form a hydrogen bond. A π–π stacking effect occurred between the pharmacophore and His41. It was shown that the residues Glu119 (bond length: 10.1 Å) and Lys134 (bond length: 8.8 Å) formed two hydrogen bond interactions with **I-4**, while four chelations (bond lengths: 5.3, 5.4, 5.9 and 6.1 Å) were shown between the **I-4** and the two manganese ions, which was the main interaction between **I-4** and the endonuclease. All these interactions helped **I-4** to anchor in the binding site of the endonuclease. In the molecular docking of baloxavir, OH in the pharmacophore and the NH_2 group on Ile-120 formed a hydrogen bond. There was a π–π stacking effect between the mother nucleus and Tyr24 and a van der Waals interaction between the mother nucleus and Glu26. The differences were that the lengths of the hydrogen bonds between baloxavir and the residues Ile-120 (bond length: 3.1 Å) of the endonuclease was shorter than that of **I-4**, which made baloxavir more tightly bound to the active site of the endonuclease than **I-4**. The binding of compound **I-4** to the enzyme had one more hydrogen bond than the binding of baloxavir to the enzyme, which could bind to the target site and interact with multiple important amino acids of the receptor with a slightly stronger interaction than baloxavir. The diphenylmethyl structure of compound **I-4** containing electron withdrawing groups with chiral centers could better bind to proteins.



Baloxavir **I-4**

Figure 8. Molecular Docking Diagram of Baloxavir and **I-4**.

The interaction between the optimal conformation of compounds **II-2** and **II-6** and the receptor protein were analyzed and compared to the molecular docking of baloxavir, as shown in Figure 9. The binding energies of compounds **II-2** and **II-6** with enzymes were −7.75 kcal/mol and −8.06 kcal/mol, respectively, surpassing the binding energies of baloxavir (−7.44 kcal/mol).



II-2 **II-6**

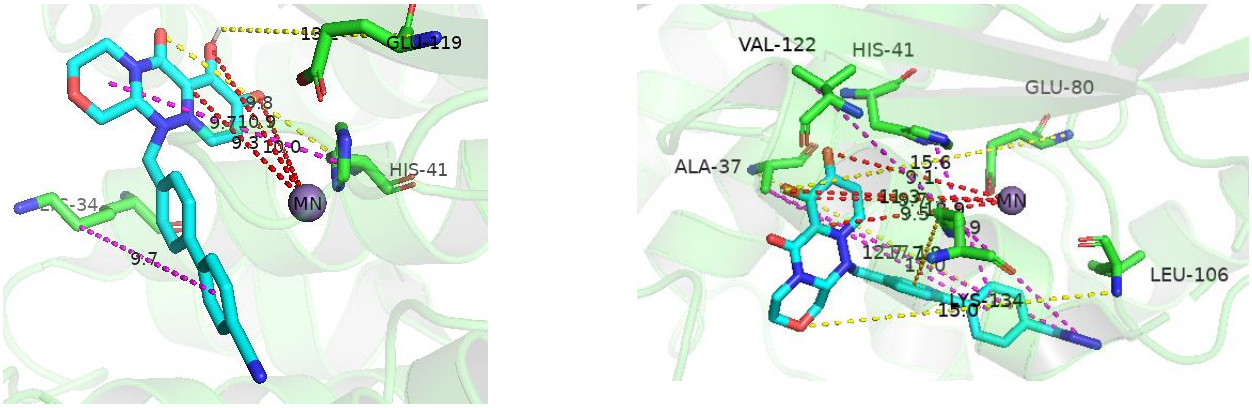
Figure 9. Molecular Docking Diagram of **II-2** and **II-6**.

In compound **II-2**, the hydroxyl (OH) group on the pharmacophore formed a hydrogen bond with the amino (NH_2) group on Glu80, while the carbonyl group formed a hydrogen bond with the NH_2 group on His41. A π–π stacking effect occurred between the dibenzocycloheptane structure and Tyr24, as well as between the pharmacophore and Lys134. The dibenzocycloheptane structure exhibited hydrophobic interaction with Ala20, Ile38, Lys34, and Ala37, and a van der Waals force was present in Glu26. The OH on the pharmacophore of compound **II-6** combined with the NH_2 group on Glu119 to form a hydrogen bond, the C=O on the pharmacophore formed a hydrogen bond with Lys134, and the F on methoxidibenzoxaheptane could also combine with the NH_2 group on Ala37 to form a hydrogen bond. A π–π stacking interaction occurred between the methoxy dibenzoxane structure and Tyr24 and His41. It had a specific hydrophobic effect with Ile38 and Ala20. There was a van der Waals interaction with Glu26.

Compound **II-2** had one more hydrogen bond and one more van der Waals force than baloxavir, and compound **II-6** had two more hydrogen bonds and one more van der Waals force than baloxavir. It was shown that the residues Glu80 (bond length: 10.6 Å) and His41 (bond length: 5.2 Å) formed two hydrogen bond interactions with **II-2**, while four chelations (bond lengths: 4.1, 4.2, 4.2 and 4.3 Å) were shown between **II-2** and the two manganese ions, which was the main interaction between **II-2** and the endonuclease.

The residues Glu119 (bond length: 12.3 Å) and Lys134 (bond length: 3.6 Å) formed two hydrogen bond interactions with **II-6**, while four chelations (bond lengths: 6.0, 7.3, 8.4 and 8.4 Å) were shown between the **II-6** and the two manganese ions, which was the main interaction between **II-6** and the endonuclease. All these interactions helped **II-2** and **II-6** to anchor in the binding site of the endonuclease. Compounds **II-2** and **II-6** could better bind to the target site and interact with multiple important amino acids of the receptor, with better interactions than baloxavir.

The optimal conformation of compounds **III-5** and **III-8** and their interaction with the receptor protein were analyzed and compared with baloxavir molecular docking, as shown in Figure 10. The binding energies of compounds **III-5** and **III-8** with enzymes were −7.54 kcal/mol and −8.64 kcal/mol, respectively, greater than the binding energies of baloxavir (−7.44 kcal/mol). The OH on the pharmacophore of compound **III-5** combined with NH2 on Glu119 to form a hydrogen bond, while C=O and O also combined with His41 to form a hydrogen bond. The biphenyl structure of **III-5** formed a cation π force with Lys34. Compound **III-8** combined OH on the pharmacophore with NH_2 on Glu80 to form a hydrogen bond, and O could also combine with NH_2 on Leu106 to form a hydrogen bond. In addition, tetrazole could also combine with NH_2 on Ala37 to form a hydrogen bond. A π-π stacking interaction between the biphenyltetrazole structure and His41, a certain hydrophobic interaction with Vai122, and a cation π interaction force with Lys134 were seen.



III-5 **III-8**

Figure 10. Molecular Docking Diagram of **III-5** and **III-8**.

Compound **III-5** had one more hydrogen bond than bloxavir, and compound **III-8** had two more hydrogen bonds and one more Van der Waals force than baloxavir. It was shown that the residues Glu119 (bond length: 13.2 Å) and His41 (bond length: 9.8 Å) formed two hydrogen bond interactions with **III-5**, while three chelations (bond lengths: 9.7, 10.0 and 10.9 Å) were shown between **III-5** and the one manganese ion, which was the main interaction between **III-5** and the endonuclease. The residues Glu80 (bond length: 15.6 Å) and Leu106 (bond length: 15.0 Å) formed two hydrogen bond interactions with **III-8**, while three chelations (bond lengths: 8.9, 9.1 and 9.7 Å) were shown between the **III-8** and the one manganese ion, which was the main interaction between **III-8** and the endonuclease. All these interactions helped **III-5** and **III-8** to anchor in the binding site of the endonuclease. **III-5** and **III-8** could better bind to the target site and interact with multiple important amino acids of the receptor, with the interaction being better than that of baloxavir. Compound **III-8** contained a biphenyltetrazolium structure, which was more conducive to binding to proteins.

Through molecular docking analysis, it can be seen that diphenylcarbinol structures can bind well to receptor proteins, and diphenylcarbinol containing electron-absorbing groups were more conducive to binding to receptor proteins. The affinity results of compound **I-4** for endonucleases show that diphenylcarbinol structures can effectively bind to

cap-dependent endonucleases. It can also be seen from the IC50 value of endonucleases that diphenylcarbinol compounds containing chiral centers were more advantageous in interacting with endonucleases. The results of the endonuclease inhibition activity of compound **I-4** were consistent with those of molecular docking. The above analysis indicated that the dibenzothiepin of baloxavir was replaced by diphenylmethyl with an electron-absorbing group and a chiral center was beneficial for enhancing the inhibition of endonuclease.

From the molecular docking results of compounds **II-2** and **II-6** with the receptor protein, it can be seen that the binding energy of the target compounds of the **II** series with the receptor protein was slightly smaller than that of baloxavir, indicating that when the sulfur atom in the dibenzothiepin structure of the baloxavir was replaced by an oxygen atom, a C–C single bond, or a C=C double bond, it could bind well with the receptor protein. At the same time, from the affinity results of compounds **II-2** and **II-6** for endonucleases, it can be seen that dibenzocycloheptane and dibenzoxaheptane structures were conducive to the binding of pharmacophores to endonucleases. It can be seen from the inhibition of endonuclease activity that dibenzocycloheptane and dibenzoxaheptane were beneficial to combine with the endonuclease and play an inhibitory role, among which dibenzocycloheptane had a better inhibitory effect on the endonuclease. The inhibitory activity results of compounds **II-2** and **II-6** were consistent with those of molecular docking. The above analysis showed that when the dibenzothiepin of baloxavir was replaced by dibenzocycloheptane and dibenzoxaheptane, it was beneficial to enhance the inhibitory effect of the compound on the activity of the endonuclease and different positions of dibenzoxaheptane structure substituents had little impact on the inhibitory effect of endonuclease activity.

From the molecular docking study results, it can be seen that compounds **III-5** and **III-8** had a lower binding energy with the receptor protein than baloxavir. This indicated that when the diphenylthiazide structure of baloxavir was replaced by a five-membered heterocycle, it could also bind well with the protein. Compound **III-8**, containing a tetrazole structure, demonstrated enhanced receptor protein binding. Affinity results for compounds **III-5** and **III-8** with endonucleases showed that the five-membered heterocyclic structure was conducive to the binding of pharmacophores to cap-dependent endonucleases. From the inhibition of endonuclease activity, it can be seen that compounds **III-5** and **III-8** had a strong endonuclease inhibitory activity. This further confirmed that the tetrazole structure was conducive to enhancing endonuclease inhibition.

3.5. Structure–Activity Relationship

According to the literature reports, molecular docking results and endonuclease inhibition findings, the structure–activity relationship was obtained.

Replacing the dibenzothiepin of baloxavir with a diphenylmethyl structure containing electron-withdrawing groups enhanced endonuclease inhibition, and the diphenylmethyl structure containing electron-absorbing groups with chiral centers was more conducive to enhancing the inhibition of endonuclease by compounds.

The dibenzothiepin of baloxavir was replaced by dibenzocycloheptane and dihydrodibenzo[b,e]oxepin structures which was beneficial to the enhancement of endonuclease inhibition and the different positions on dihydrodibenzo[b,e]oxepin structures exerting a small effect on endonuclease activity. Meanwhile, according to the literature, the novel substituted polycyclic pyridinone derivatives obtained by optimizing the structure of dibenzothiepin showed strong anti-influenza virus activity and low cytotoxicity against influenza virus (HIN1).

The dibenzothiepin of baloxavir was replaced by five-membered heterocyclic structures containing aryl substituents which could enhance the inhibition of the endonuclease. Conversely, replacing the dibenzothiepin of baloxavir with a single five-membered heterocyclic structure diminished endonuclease inhibition.

A structure−activity relationship study revealed that when dibenzothiepin of baloxavir was replaced by a diphenylmethyl structure containing electron-withdrawing groups, no groups were introduced to the dibenzocycloheptene ring or dibenzocycloheptane ring, and

benzothiepin containing a five-membered heterocyclic ring and dihydrodibenzo[b,e]oxepin structures was employed, the antiviral activity was the best.

4. Conclusions

The pharmacodynamic group and pharmacological action of baloxavir were analyzed to study the derivatives of baloxavir. In total, 3 series of 21 unreported compounds were designed and synthesized. Molecular docking, PAINS-remover and SwissADME procedures were used to verify the design rationality, and the cap-dependent endonuclease activity inhibition and affinity of these target compounds were evaluated. The inhibitory activities of compound **I-4**, series **II** target compounds (**II-1~II-9**) and compound **III-8** against cap-dependent endonuclease were similar to those of baloxavir (7.45 μM), and especially compounds **I-4** (3.29 μM) and **II-2** (1.46 μM) showed strong cap-dependent endonuclease inhibitory activities. The structure–activity relationship was concluded through the activity study. When the dibenzothiepin fragment of baloxavir was replaced by diphenylmethyl, dibenzocycloheptane, dihydrodibenzo[b,e]oxepin, and 5-membered heterocyclic compounds containing aryl substitutions, the inhibition of endonuclease was enhanced.

Supplementary Materials: The following supporting information can be downloaded at https://www.mdpi.com/article/10.3390/cryst13070988/s1. Table S1: Composition and concentration of reaction group and control group; Table S2: Composition and concentration of reaction group and control group; Experimental data of related compounds.

Author Contributions: Conceptualization, Y.W., Z.Z. and Z.X.; methodology, Y.W. and Z.X.; software, Y.W. and L.C.; validation, Y.W. and L.C.; formal analysis, Y.W. and L.C.; investigation, Y.W. and J.W.; resources, Z.M., J.L. and H.W.; data curation, H.W., J.L. and J.W.; writing—original draft preparation, Y.W.; writing—review and editing, Y.W., Z.Z. and Z.X.; visualization, Y.W. and Z.X.; supervision, Y.W., Z.Z. and Z.X.; project administration, Z.M., Z.Z. and Z.X.; funding acquisition, Z.Z. and Z.M. All authors have read and agreed to the published version of the manuscript.

Funding: This research received no external funding.

Institutional Review Board Statement: Not applicable.

Informed Consent Statement: Not applicable.

Data Availability Statement: Not applicable.

Acknowledgments: Thanks to the Analysis and Testing Center of the Beijing Institute of Technology for providing structural testing services such as nuclear magnetic resonance and mass spectrometry.

Conflicts of Interest: The authors declare no conflict of interest.

References

1. Gao, Y.; Liu, Z.; Li, Z. Research Progress in Anti Influenza Virus Drugs. *China Med. Biotechnol.* **2015**, *10*, 533–539.
2. Thompson, W.W.; Weintraub, E.; Dhankhar, P.; Cheng, P.-Y.; Brammer, L.; Meltzer, M.I.; Bresee, J.S.; Shay, D.K. Estimates of US influenza-associated deaths made using four different methods. *Influenza Other Respir. Viruses* **2009**, *3*, 37–49. [CrossRef]
3. Pleschka, S. Overview of influenza viruses. *Curr. Top. Microbiol. Immunol.* **2013**, *370*, 1–20.
4. Xu, S.; He, X.; Chen, C.; Tian, H. Research Progress in Anti Influenza Virus Drugs. *Mod. Drugs Clin.* **2009**, *24*, 65–70.
5. Cheng, N.; Chen, B.; Wang, Y. A new oral anti influenza drug-Oseltamivir. *Chin. J. Clin. Pharm.* **2002**, *11*, 55–59.
6. Gu, J. Research progress of Peramivir, a novel potent neuraminidase inhibitor against influenza virus. *Chin. J. New Drugs* **2013**, *22*, 989–997.
7. Zhang, Q.; Zhao, Q.; Xiong, R.; Li, J.-F.; Shen, J.-S. Research progress of anti-influenza virus agents. *Acta Pharm. Sin.* **2010**, *45*, 289–299.
8. von Itzstein, M. The war against influenza: Discovery and development of sialidase inhibitors. *Nat. Rev. Drug Discov.* **2007**, *6*, 967–974. [CrossRef]
9. Hu, Y.; Hau, R.K.; Wang, Y.; Tuohy, P.; Zhang, Y.; Xu, S.; Ma, C.; Wang, J. Structure-property relationship studies of Influenza A virus AM2-S31N proton channel blockers. *ACS Med. Chem. Lett.* **2018**, *9*, 1111–1116. [CrossRef]
10. Das, K. Antivirals targeting influenza A virus. *J. Med. Chem.* **2012**, *55*, 6263–6277. [CrossRef]

11. Guti Rrze, R.A.; Naughtin, M.; Horm, S.V.; San, S.; Buchy, P. A (H5N1) virus evolution in South East Asia. *Viruses* **2009**, *1*, 335–361. [CrossRef]
12. Xu, Y.; Meng, X.; Zhang, Y. Clinical research progress of anti influenza virus drugs with different mechanisms of action. *Shanghai Pharm.* **2014**, *35*, 58–60.
13. Pizzorno, A.; Abed, Y.; Boivin, G. Influenza drug resistance. *Semin. Respir. Crit. Care Med.* **2011**, *32*, 409–422. [CrossRef] [PubMed]
14. McMichael, A.J.; Haynes, B.F. Influenza vaccines: mTOR inhibition surprisingly leads to protection. *Nat. Immunol.* **2013**, *14*, 1205–1207. [CrossRef]
15. Chen, S.; Zhong, W. A novel neuraminidase inhibitor—Anti influenza drug AV5080. *J. Clin. Drug Ther.* **2018**, *16*, 19–21.
16. Herlocher, M.L.; Truscon, R.; Elias, S.; Yen, H.-L.; Roberts, N.A.; Ohmit, S.E.; Monto, A.S. Influenza viruses resistant to the antiviral drug oseltamivir: Transmission studies in ferrets. *J. Infect. Dis.* **2004**, *190*, 1627–1630. [CrossRef] [PubMed]
17. Ivachtchenko, A.V.; Ivanenkov, Y.A.; Mitkin, O.D.; Yamanushkin, P.M.; Bichko, V.V.; Shevkun, N.A.; Karapetian, R.N.; Leneva, I.A.; Borisova, O.V.; Veselov, M.S. Novel oral anti-influenza drug candidate AV5080. *J. Antimicrob. Chemother.* **2014**, *69*, 1892–1902. [CrossRef]
18. Heo, Y.A. Baloxavir: First global approval. *Drugs* **2018**, *78*, 693–697. [CrossRef]
19. Sun, C.; Qiao, H. A new oral anti-influenza drug: Baloxavir marboxil. *Chin. J. New Drugs Clin. Remed.* **2019**, *38*, 262–267.
20. Li, C.; Chen, H. Enhancement of influenza virus transmission by gene reassortment. *Curr. Top. Microbiol. Immunol.* **2014**, *385*, 185–204.
21. Tao, J.; Lv, Q.; Li, X.; Dai, P.; Ye, Y.; Shen, Z. Research on new anti-influenza drug baloxavir marboxil. *Chin. J. Clin. Med.* **2019**, *26*, 308–311.
22. Baker, D.E. Baloxavir marboxil. *Hosp. Pharm.* **2019**, *54*, 165–169. [CrossRef] [PubMed]
23. Kawaguchi, N.; Koshimichi, H.; Ishibashi, T.; Wajima, T. Evaluation of drug-drug interaction potential between baloxavir marboxil and oseltamivir in healthy subjects. *Clin. Drug Investig.* **2018**, *38*, 1053–1060. [CrossRef]
24. Hayden, F.G.; Sugayan, N.; Hirotsu, N.; Lee, N.; de Jong, M.D.; Hurt, A.C.; Ishida, T.; Sekino, H.; Yamada, K.; Portsmouth, S.; et al. Baloxavir marboxil for uncomplicated in fluenza in adults andadolescents. *N. Engl. J. Med.* **2018**, *379*, 913–923. [CrossRef]
25. Omoto, S.; Speranzini, V.; Hashimoto, T.; Noshi, T.; Yamaguchi, H.; Kawai, M.; Kawaguchi, K.; Uehara, T.; Shishido, T.; Naito, A.; et al. Characterization of influenza virus variants induced by treatment with the endonuclease inhibitor baloxavir marboxil. *Sci. Rep.* **2018**, *8*, 9633. [CrossRef]
26. Tang, C.; Ren, Q.; Luo, H.; Yin, J.; Yi, K.; Lei, Y.; Wang, Y.; Zhang, Y. Influenza Virus Replication Inhibitors and Their Uses. International Patent (PCT/CN2018/106092) WO2019/052565A1, 21 March 2019.
27. Tang, L.; Yan, H.; Wu, W.; Chen, D.; Gao, Z.; Hou, J.; Zhang, C.; Jiang, Y. Synthesis and anti-influenza virus effects of novel substituted polycyclic pyridone derivatives modified from baloxavir. *J. Med. Chem.* **2021**, *64*, 14465–14476. [CrossRef]
28. Miyagawa, M.; Akiyama, T.; Taoda, Y.; Takaya, K.; Takahashi Kageyama, C.; Tomita, K.; Yasuo, K.; Hattori, K.; Shano, S.; Yoshida, R.; et al. Synthesis and SAR study of carbamoyl pyridone bicycle derivatives as potentinhibitors of influenza cap-dependent endonuclease. *J. Med. Chem.* **2019**, *62*, 8101–8114. [CrossRef] [PubMed]

Disclaimer/Publisher's Note: The statements, opinions and data contained in all publications are solely those of the individual author(s) and contributor(s) and not of MDPI and/or the editor(s). MDPI and/or the editor(s) disclaim responsibility for any injury to people or property resulting from any ideas, methods, instructions or products referred to in the content.